PAPER

Excess-Bandwidth Transmit Filtering Based on Minimization of Variance of Instantaneous Transmit Power for Low-PAPR SC-FDE

Amnart BOONKAJAY[†a)], *Student Member*, Tatsunori OBARA[†], Tetsuya YAMAMOTO[†], *Members*, and Fumiyuki ADACHI[†], *Fellow*

SUMMARY   Square-root Nyquist transmit filtering is typically used in single-carrier (SC) transmission. By changing the filter roll-off factor, the bit-error rate (BER), peak-to-average power ratio (PAPR), and spectrum efficiency (SE) changes, resulting in a tradeoff among these performance indicators. In this paper, assuming SC with frequency-domain equalization (SC-FDE), we design a new transmit filtering based on the minimum variance of instantaneous transmit power (VIP) criterion in order to reduce the PAPR of the transmit signal of SC-FDE. Performance evaluation of SC-FDE using the proposed transmit filtering is done by computer simulation, and shows that the proposed transmit filtering contributes lower transmit PAPR, while there exists only a small degradation in BER performance compared to SC-FDE using square-root Nyquist filtering.

key words: *single-carrier transmission, transmit filtering, peak-to-average power ratio (PAPR)*

1. Introduction

High-speed and high-quality are the main requirements for the next-generation mobile network [1]. However, an existence of multipath propagation with several time delays results in a frequency-selective fading channel, where the transmission performance in terms of bit-error rate (BER) degrades [2]. Orthogonal frequency division multiplexing (OFDM) is introduced as a promising transmission technique which is robust against frequency selectivity, but its high peak-to-average power ratio (PAPR) of transmit signal is the main drawback [3]. On the other hand, single-carrier transmission with frequency-domain equalization (SC-FDE) [4], [5] provides good performance under fading environment with lower PAPR, and hence, its combination with frequency division multi-access (FDMA), called SC-FDMA, has been adopted as the uplink multiple access technique in LTE system.

SC signal can be optionally generated by inserting discrete Fourier transform (DFT) into conventional OFDM transmitter [6]. By employing such this approach, frequency-domain signal processing, where transmit and receive filtering can be done as simple one-tap multiplication, is approachable [7]. Additional signal manipulation, e.g. frequency mapping, is able to be flexibly implemented.

Square-root raised cosine (SRRC) filter, one example of a square-root Nyquist filter, is typically used as a transmit

filtering in SC-FDE for limiting the transmission bandwidth [8]. Roll-off factor is introduced as a parameter controlling filter shape and extra transmission bandwidth. Effects on system performance when changing roll-off factor of SRRC as the transmit filter have been well described in [9]–[11] in many points of view. With regard to PAPR [9], a certain value of roll-off factor provides very low PAPR. In aspect of BER [10], [11], the extra bandwidth yielded by the roll-off factor provides additional diversity gain, resulting in BER improvement. It is also obvious that increasing roll-off factor degrades the spectrum efficiency (SE). As a consequence, there exists a tradeoff among these performance indicators when either filter shape or filter bandwidth changes. In this paper, low-PAPR transmission is our main objective rather than BER or SE.

There exist many studies which proposed PAPR reduction techniques based on transmit filtering and precoding design. These techniques are preferable because of low complexity and no major changes on transceiver. Some articles introduced new filter shapes which were constructed by either improving an existing conventional filter or derived from Nyquist prototype [12]–[16]. PAPR was examined for various types of conventional transmit filtering in Ref. [17], where OFDM transmission is considered. Meanwhile, the above techniques cannot guarantee the lowest PAPR. It is possible to determine a new transmit filtering providing lower PAPR than the existing filtering approaches.

Many studies also stated that employing a minimization algorithm on the definition of PAPR is far too complicated. Recently, the variance of instantaneous transmit power (VIP) was introduced as a parameter which corresponds to PAPR [18], [19]. A transmit signal with high VIP indicates its high variation of both signal amplitude and instantaneous power, resulting in high peak, and vice versa. Reference [18] also proposed a low-PAPR precoder for OFDM transmitter based on a minimum VIP (min-VIP) criterion. The algorithm proposed in Ref. [18] is also applicable with some modification to SC-FDE transmission. Note that roll-off factor is not considered in Ref. [18]. In Ref. [19], transmission with extra bandwidth (e.g. roll-off factor) is introduced, but the proposed transmit precoder does not adequately utilize the bandwidth expansion to improve both PAPR and BER performance.

The above discussions motivate us to design a frequency-domain-based transmit filtering technique providing the following contributions:

- A new transmit filtering design is introduced based on the min-VIP criterion. The PAPR performance of the designed filtering is expected to be better than using SRRC filtering, while there is no serious BER degradation.
- Similar to SRRC filtering, transmission of extra bandwidth controlled by roll-off factor is still achievable for the proposed filtering. The effect of roll-off factor on PAPR performance is also discussed.
- A benefit of excess-bandwidth transmission in terms of BER improvement is realized by employing frequency-domain spectrum copying at the transmitter and joint FDE using minimum mean-square criterion (MMSE-FDE) with spectrum combining [11]. By using this approach, additional frequency diversity gain can be obtained.
- Performance evaluations of both SC-FDE using the proposed filtering and SRRC filtering are done by computer simulation, and are shown in terms of BER and complementary cumulative distribution function (CCDF) [20] of PAPR.

This paper is organized as follows. SC-FDE transmission system model is introduced in Sect. 2. The definition of VIP corresponding to the transmitted signal is described in Sect. 3. Section 4 presents the design of low-PAPR transmit filtering based on min-VIP criterion. Section 5 shows the performance evaluations. Finally, Sect. 6 concludes the paper.

2. SC-FDE System Model

Figure 1 illustrates a single-user, single-antenna SC-FDE transmission model considered in this paper, where the transmission is assumed to be a block transmission of M symbols over available N_c subcarriers ($M \leq N_c$). We consider the baseband filtering, which can be viewed as precoding or power allocation in the frequency-domain [10], [11].
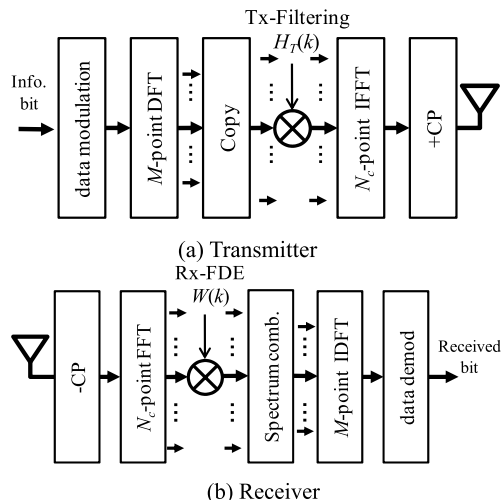

(a) Transmitter

(b) Receiver

Fig. 1 SC transmission system model.

We want to design the spectrum shape within the predefined mask (i.e., only the pre-assigned subcarriers are used).

In this paper, we consider the case of the roll-off factor $\alpha \leq 1$ since it is more practical especially when the transmission bandwidth is limited. Therefore, the maximum number of available subcarriers is $N_c=2M$. This also indicates that all $N_c=2M$ subcarriers are used when roll-off factor $\alpha=1$. As the spectrum mask is narrowed, a lower value of α needs to be used and hence, the number of subcarriers to be used is reduced.

2.1 Transmitter

A transmission block consisting of M modulated symbols is represented by a vector $\mathbf{d} = [d(0), d(1), \ldots, d(M-1)]^T$. The block $\mathbf{d}$ is firstly transformed into frequency-domain components, and then those frequency components are copied to the entire N_c subcarriers (assuming $N_c = 2M$ for simplicity). Prior to this operation, a matrix $\mathbf{E}_M$ is introduced, which is a row-repeated version of M-point DFT matrix with the dimension of $N_c \times M$, that is

$$\mathbf{E}_M = \begin{bmatrix} \mathbf{f}_M(\frac{M}{2}) \\ \vdots \\ \mathbf{f}_M(M-1) \\ \mathbf{f}_M(0) \\ \vdots \\ \vdots \\ \mathbf{f}_M(M-1) \\ \mathbf{f}_M(0) \\ \vdots \\ \mathbf{f}_M(\frac{M}{2}-1) \end{bmatrix}, \tag{1}$$

where $\mathbf{f}_M(m)$ is a row vector from the m-th row of M-point DFT matrix $\mathbf{F}_M$, which is expressed by

$$\mathbf{F}_M = \frac{1}{\sqrt{M}} \begin{bmatrix} 1 & 1 & \cdots & 1 \\ 1 & e^{-j2\pi\frac{1\times 1}{M}} & \cdots & e^{-j2\pi\frac{1\times(M-1)}{M}} \\ \vdots & \vdots & \ddots & \vdots \\ 1 & e^{-j2\pi\frac{(M-1)\times 1}{M}} & \cdots & e^{-j2\pi\frac{(M-1)\times(M-1)}{M}} \end{bmatrix}, \tag{2}$$

and its Hermitian transpose $\mathbf{F}_M^H$ represents inverse operation. Next, $\mathbf{D} = [D(0), D(1), \ldots, D(N_c-1)]^T$ is determined as a frequency-domain signal vector, which is given by

$$\mathbf{D} = \mathbf{E}_M \mathbf{d}. \tag{3}$$

Transmit filtering is introduced by a matrix $\mathbf{H}_T$. $\mathbf{H}_T$ is an $N_c \times N_c$ diagonal matrix which N_c central elements in the diagonal contain transmit filter coefficients $\left\{ H_T(\frac{-N_c}{2}), \ldots, H_T(\frac{N_c}{2}-1) \right\}$. $\mathbf{H}_T$ is expressed by

$$\mathbf{H}_T = diag \left[H_T \left(\frac{-N_c}{2} \right), \ldots, H_T \left(\frac{N_c}{2} - 1 \right) \right]. \tag{4}$$

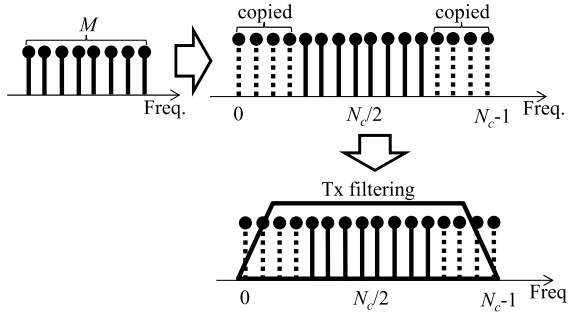In case of transmission using SRRC transmit filtering [7],

Fig. 2 Transmit filtering algorithm with excess bandwidth (assuming $\alpha=1$).

the filter coefficients $H_T(k)$ can be determined by

$$H_T(k) = \begin{cases} 1, & 0 \leq |k| < \frac{1-\alpha}{2} M \\ \cos(\frac{\pi}{2\alpha M}(|k| - \frac{1-\alpha}{2}M)), & \frac{1-\alpha}{2}M \leq |k| < \frac{1+\alpha}{2}M \\ 0, & \text{otherwise} \end{cases} \quad (5)$$

Instead of SRRC transmit filter coefficients, the set of coefficients $\left\{H_T(\frac{-N_c}{2}), \ldots, H_T(\frac{N_c}{2} - 1)\right\}$ in Eq. (4) can be changed to a set of filter coefficients of the proposed low-PAPR transmit filtering. The method of obtaining those filter coefficients is discussed in more details in Sect. 4.

After that, the filtered signal is transformed back into time domain by N_c-point inverse fast Fourier transform (IFFT) matrix $\mathbf{F}_{N_c}^H$. Time-domain signal $\mathbf{s} = [s(0), s(1), \ldots, s(N_c - 1)]^T$ after passing through all processes can be expressed as

$$\mathbf{s} = \mathbf{F}_{N_c}^H \mathbf{H}_T \mathbf{D} = \mathbf{F}_{N_c}^H \mathbf{H}_T \mathbf{E}_M \mathbf{d}. \quad (6)$$

Finally, the last N_g samples of transmit block are copied as a cyclic prefix (CP) and inserted into the guard interval (GI), then a CP-inserted signal block of $N_g + N_c$ samples is transmitted.

The transmit filtering algorithm, with particular roll-off factor α, is illustrated by Fig. 2. It can be seen that $H_T(k)$ is applied to $D(k)$ as one-tap multiplication.

2.2 Receiver

The transmission is conducted under L-path independent block Rayleigh fading channel [2]. Channel response is given by

$$h(\tau) = \sum_{l=0}^{L-1} h_l \delta(\tau - \tau_l), \quad (7)$$

where h_l and τ_l are complex-valued path gain and time delay of the l-th path, respectively. $\delta(\cdot)$ is the delta function. The received signal after CP removal, $\mathbf{r} = [r(0), r(1), \ldots, r(N_c - 1)]^T$, is

$$\mathbf{r} = \sqrt{\frac{2E_s}{T_s}} \mathbf{h}\mathbf{s} + \mathbf{n}, \quad (8)$$

where E_s and T_s are symbol energy and symbol duration,

respectively. $\mathbf{s}$ is obtained from (6), and $\mathbf{n}$ is noise vector in which element is zero-mean additive white Gaussian noise (AWGN) having the variance $2N_0/T_s$ with N_0 being the one-sided noise power spectrum density. In addition, channel response matrix $\mathbf{h}$ is a circular matrix representing time-domain channel impulse response, which is

$$\mathbf{h} = \begin{bmatrix} h_0 & & h_{L-1} & \cdots & h_1 \\ h_1 & \ddots & & \ddots & \vdots \\ \vdots & & h_0 & \mathbf{0} & h_{L-1} \\ h_{L-1} & h_1 & \ddots & & \\ & \ddots & \vdots & & \ddots \\ \mathbf{0} & h_{L-1} & \cdots & \cdots & h_0 \end{bmatrix}. \quad (9)$$

The received signal is transformed into frequency domain by N_c-point FFT, obtaining the frequency-domain received signal $\mathbf{R}$ as

$$\begin{aligned} \mathbf{R} &= \sqrt{\frac{2E_s}{T_s}} \mathbf{F}_{N_c} \mathbf{h}\mathbf{s} + \mathbf{F}_{N_c} \mathbf{n} \\ &= \sqrt{\frac{2E_s}{T_s}} \mathbf{F}_{N_c} \mathbf{h}\mathbf{F}_{N_c}^H \mathbf{H}_T \mathbf{D} + \mathbf{F}_{N_c} \mathbf{n}, \\ &= \sqrt{\frac{2E_s}{T_s}} \mathbf{H}_c \mathbf{H}_T \mathbf{D} + \mathbf{N} \end{aligned} \quad (10)$$

where the frequency-domain channel response $\mathbf{H}_c$ is

$$\mathbf{F}_{N_c} \mathbf{h}\mathbf{F}_{N_c}^H = diag [H_c(0), \ldots, H_c(N_c - 1)] \equiv \mathbf{H}_c. \quad (11)$$

Joint MMSE-FDE with spectrum combining is later employed in order to mitigate the effect of fading channel and recover the original M frequency-domain components with additional frequency diversity gain. In this paper, an $M \times N_c$ matrix $\mathbf{W}$ represents this operation and $\mathbf{W}$ is expressed by Eq. (12), where $W(k), k = 0 \sim N_c - 1$ is determined so as to minimize the mean-square error (MSE) between $\mathbf{D}$ and the frequency-domain signal after equalization $\hat{\mathbf{D}}=\mathbf{W}\mathbf{R}$ by referencing Ref. [11], and given by

$$W(k) = \frac{\hat{H}^*(k)}{\displaystyle\sum_{g=0}^{1} \left|\hat{H}(k \bmod M + gM)\right|^2 + \left(\frac{E_s}{N_0}\right)^{-1}}, \quad (13)$$

where $\hat{H}(k) = H_c(k)H_T(k)$ and $H_c(k)$ is the elements in $\mathbf{H}_c$ with respect to each frequency index. In Ref. [11], the receiver employs the SRRC filter (i.e. matched filter) as the receive filter, which is followed by the MMSE filter. In this paper, however, the MMSE-FDE is designed to include the receive filter function. This is the reason why the numerator of Eq. (13) becomes $H_c^*(k)H_T^*(k)$.

The frequency-domain received signal after equalization and spectrum combining $\hat{\mathbf{D}}$ is finally transformed back into time-domain received signal before demodulation $\hat{\mathbf{d}} = [\hat{d}(0), \hat{d}(1), \ldots, \hat{d}(M - 1)]^T$ as

$$\hat{\mathbf{d}} = \mathbf{F}_M^H \hat{\mathbf{D}} = \mathbf{F}_M^H \mathbf{W}\mathbf{R}. \quad (14)$$

In addition, spectrum combining is simply depicted by

$$\mathbf{W} = \begin{bmatrix} & & W(\frac{N_c}{4}) & & & & & & & W(\frac{3N_c}{4}) & & \\ \mathbf{0} & & & \ddots & & & & & & & \ddots & \\ & & & & W(\frac{N_c}{2}-1) & & & & & & & W(N_c-1) \\ W(0) & & & & & W(\frac{N_c}{2}) & & & & & & \\ \ddots & & & & & & \ddots & & & & \mathbf{0} & \\ & W(\frac{N_c}{4}-1) & & & & & & W(\frac{3N_c}{4}-1) & & & & \end{bmatrix} \tag{12}$$

Fig. 3 Spectrum combining.

Fig. 3. It can be seen both from Eq. (12) and the figure that spectrum combining should be done corresponding to the copying at the transmitter, otherwise the frequency diversity is not achieved.

3. VIP Definition

It is previously mentioned that either a closed-form definition or other matrics relating to PAPR should be available for determining a low-PAPR transmit filtering. In this paper, Refs. [17], [18] are used as a guideline for the definition of VIP for SC-FDE. Then, the derived VIP is used for designing the low-PAPR transmit filtering in the next section.

The method of VIP determination begins from the time-domain transmit signal vector **s** whose each component is represented by $s(n), n = 0 \sim N_c - 1$, as shown in Eq. (6). An overall transmit operation matrix $\mathbf{X} = \mathbf{F}_{N_c}^H \mathbf{H}_T \mathbf{E}_M$ is also defined to simplify the derivation. Then, Eq. (6) is rewritten as $\mathbf{s} = \mathbf{Xd}$, where each element $s(n)$ is given by

$$s(n) = \sum_{m=0}^{M-1} x_{nm} d(m). \tag{15}$$

Here, x_{nm} represents an element in **X** at the n-th row and m-th column.

By the definition, instantaneous transmit power of each sample is $|s(n)|^2$. The VIP of a particular transmission block, represented by σ^2, is then given by

$$\sigma^2 = \frac{1}{N_c} \sum_{n=0}^{N_c-1} E\left[\left| |s(n)|^2 - E[|s(n)|^2] \right|^2 \right]. \tag{16}$$

Note that $E[\cdot]$ represents an ensemble averaging. It can be observed that $E[|s(n)|^2]$ is indeed an averaged transmit power over a block (hereinafter represented by P_{avg}). With some simple manipulations, Eq. (16) is rewritten as

$$\sigma^2 = \frac{1}{N_c} \sum_{n=0}^{N_c-1} E[|s(n)|^4] - P_{avg}^2. \tag{17}$$

Assuming that all transmission blocks are independent, substituting Eq. (15) into Eq. (17) yields the VIP

$$\sigma^2 = \frac{1}{N_c} \sum_{n=0}^{N_c-1} \left[2 \left[\sum_{m=0}^{M-1} |x_{nm}|^2 \right]^2 - (2-\kappa) \sum_{m=0}^{M-1} |x_{nm}|^4 \right] - P_{avg}^2. \tag{18}$$

Note that the derivation of Eq. (18) is in Appendix-A. The term $\kappa = E[|d(m)|^4]$ in Eq. (18) indicates that the VIP, and further the PAPR, depends on modulation type. We assume that $\{d(m)\}$ are independent and identically distributed (i.i.d.) for simplicity. In case of constant-amplitude modulation, $\kappa = 1$.

It can be also observed that the derived VIP σ^2 given by Eq. (18) is similar to one in Refs. [17], [18] even though they are operated in different transmission schemes. This is because they both are derived from the overall transmit poeration matrix **X**. However, the structure of **X**, including the value of x_{nm}, of each transmission scheme is not the same.

4. Design of Low-PAPR Transmit Filtering

In this section, the derived VIP in the previous section is used as a criterion for determining a low-PAPR transmit filtering for SC-FDE.

4.1 Problem Formulation

We are also interested in other optimization techniques, especially non-iterative optimization since it requires lower computational complexity. However, the optimization problem needs to be relaxed as much as possible since it involves with many variables as understood from Eq. (18). In this paper, we alternatively focus on iterative optimization, where the simplification of Eq. (18) is not required. Firstly, an $N_c \times M$ transmit precoder **P** is introduced as

$$\mathbf{P} = \mathbf{H}_T \mathbf{E}_M. \tag{19}$$

$$\arg \min_{\{H_T(k)\}} \sigma^2 = \frac{1}{N_c} \sum_{n=0}^{N_c-1} \left[2 \left[\sum_{m=0}^{M-1} |x_{nm}|^2 \right]^2 - (2-\kappa) \sum_{m=0}^{M-1} |x_{nm}|^4 \right] - P_{avg}^2$$

$$\text{s.t. } \frac{1}{M} \sum_{k=0}^{N_c-1} |H_T(k)|^2 = 1, \text{ and } H_T(k) \geq 0 \; \forall k \tag{20}$$

By using Eq. (19), complexity of min-VIP problem solution is possibly reduced since the problem is determined in precoder-level.

The min-VIP problem is formulated as Eq. (20). The minimization problem in Eq. (20) is similar to one in Ref. [18]. However, it is observed from Refs. [18], [19] that an optimal set of transmit filter coefficients is real and positive even though only transmit power constraint is employed. Note that the minimization of VIP problem in Ref. [18] considers OFDM transmission without roll-off factor, while Ref. [19] considers SC-FDE transmission with bandwidth expansion, where the starting point of gradient search algorithm is ideal rectangular filter and the excess bandwidth is not utilized (therefore, an additional for obtaining frequency diversity is not obtained).

Meanwhile, it is discussed in Ref. [19] that the minimization of VIP always converges to one solution if the frequency-domain filter coefficients are kept positive. Even though it is not explained in Refs. [18], [19] how the constraint of non-negative filter coefficients affects PAPR performance and that the constraint of non-negative is not mandatory, we have tried to employ the constraint that the transmit filter coefficients should be greater than or equal to zero in the minimization problem in order to confirm a unique solution, especially when the starting point of gradient search in our paper is different from Refs. [18], [19] (i.e. Refs. [18], [19] use ideal rectangular filter as a starting point while our paper uses the SRRC filter as a starting point). Note that the method of selecting the starting point is discussed in details in Sect. 4.2.

Equation (20) can be rewritten by referencing Eq. (19) as

$$\arg \min_{\mathbf{P}} \sigma^2 = \frac{1}{N_c} \sum_{n=0}^{N_c-1} \left[2 \left[\sum_{m=0}^{M-1} |x_{nm}|^2 \right]^2 - (2-\kappa) \sum_{m=0}^{M-1} |x_{nm}|^4 \right] - P_{avg}^2. \tag{21}$$

The following transmit power constraint is introduced:

$$\frac{1}{M} \sum_{k=0}^{N_c-1} |H_T(k)|^2 = 1. \tag{22}$$

If the precoder in Eq. (19) is considered, the transmit power constraint in Eq. (22) is rewritten as $|\mathbf{p}_m|^2 = 1$, where $\mathbf{p}_m$ is an m-th column vector of $\mathbf{P}$.

4.2 Solving the Min-VIP Problem

The minimization problem in Eq. (20) or Eq. (21) are non-convex, and hence direct solving may be too difficult. Alternatively, the problems can be solved by numerical methods; gradient search algorithm [21] is an example among them.

We select Eq. (21) as the min-VIP problem to be solved in this section. Prior to problem solving, gradient function should exist. The gradient function with respect to $\mathbf{p}_m$ is determined by

$$\nabla_{\mathbf{p}_m} \sigma^2 = \nabla_{\mathbf{p}_m, \text{real}} \sigma^2 + j \nabla_{\mathbf{p}_m, \text{img}} \sigma^2. \tag{23}$$

The reason of using gradient of $\mathbf{p}_m$ instead of either $\mathbf{P}$ or $\mathbf{H}_T$ is the transmit power constraint (as shown in Eq. (22)) can be simply controlled as a vector normalization. Substituting Eq. (18) in Eq. (23) yields

$$\nabla_{\mathbf{p}_m} \sigma^2 = \frac{4}{N_c} \sum_{n=0}^{N_c-1} \left[2 \left(\left[\sum_{l=0}^{M-1} |x_{nl}|^2 \right]^2 \right) - (2-\kappa)(|x_{nm}|^2) \right] (x_{nm} \mathbf{e}_n^H), \tag{24}$$

where

$$\mathbf{e}_n = \frac{1}{N_c} \left[e^{(j2\pi(\frac{N_c-J}{2})(n)}{N_c})}, \ldots, e^{(j2\pi(\frac{N_c+J}{2}-1)(n)}{N_c})} \right]. \tag{25}$$

The derivation of Eq. (24) is shown in Appendix-B.

Gradient search is employed iteratively for each column in $\mathbf{P}$, i.e. $\mathbf{p}_m, m = 0, \ldots, M-1$. The searching algorithm at the t-th iteration is expressed by

$$\tilde{\mathbf{p}}_m[t+1] = \mathbf{p}_m[t] - \gamma \nabla_{\mathbf{p}_m[t]} \sigma^2, \tag{26}$$

where γ represents the step-size parameter. Then $\tilde{\mathbf{p}}_m[t+1]$ is normalized as

$$\mathbf{p}_m[t+1] = \frac{\tilde{\mathbf{p}}_m[t+1]}{|\tilde{\mathbf{p}}_m[t+1]|}. \tag{27}$$

One important thing for iterative gradient search is the starting point, i.e. $\mathbf{p}_m[0]$. The search algorithm with a good starting point requires a smaller number of iterations. In Ref. [18], a corresponding column of DFT matrix is selected as a starting point, which refers to original SC-FDE. However, the filter coefficients are obtained before transmission by solving the minimization problem using a gradient search algorithm and the same filter coefficients are used for all succeeding block transmissions. Therefore, there is no need to

concern about the number of iterations.

Our goal is to find the transmit filtering which provides a low PAPR than conventional filtering. The SRRC filter coefficients are selected as the starting point; i.e., $\mathbf{P} = \mathbf{H}_{T,\text{SRRC}}\mathbf{E}_M$ where $\mathbf{H}_{T,\text{SRRC}}$ represents SRRC filtering matrix. By referencing to Refs. [11]–[17], the SRRC transmit filtering provides a very-low PAPR compared to other conventional filters. If another conventional filtering is used as the starting point, the result from gradient search algorithm may not guarantee for achieving lower PAPR than SRRC filtering.

4.3 Obtaining Transmit Filter Coefficients

An optimum precoder $\mathbf{P}_{opt}$ is determined after particular iterations of Eqs. (26) and (27). An inverse operation of Eq. (19) is employed in order to obtain an optimum transmit filtering matrix $\mathbf{H}_{T,opt}$, where optimum filter coefficients are contained inside. That is

$$\mathbf{H}_{T,opt} = \mathbf{P}_{opt}\mathbf{E}_M^+, \qquad (28)$$

where $\mathbf{E}_M^+$ represents Moore-Penrose pseudoinverse of $\mathbf{E}_M$ [22]. Note that the filter coefficients obtained from Eq. (28) can be used in all block transmissions since κ can be statistically determined as the same value for each transmission symbol, but still depends on the modulation type.

5. Performance Evaluation

Numerical and simulation parameters are summarized in Table 1. We assume quadrature phase-shift keying (QPSK) or 16-quadrature amplitude modulation (16-QAM) block transmissions with the number of available subcarriers N_c=512. Channel coding is not considered. The propagation channel is assumed to be a frequency-selective block Rayleigh fading channel having a symbol-spaced L=16-path uniform power delay profile. Note that the parameters for gradient search algorithms (i.e. the number of iterations and step-size parameter) are determined so as to guarantee the convergence. The step-size parameter γ=1.0 and the number of iterations equals 100 are used (see Appendix-C). The guard interval for the cyclic-prefix insertion can be utilized as the symbol timing recovery and the frequency offset estimation in SC-FDE. Here, ideal symbol timing recovery and no frequency offset are assumed in this paper.

5.1 Filter Impulse Response and Transfer Function

Filter impulse responses and transfer functions of both SRRC and the low-PAPR filters are discussed in this subsection. Figure 4 shows the frequency-domain transfer functions of SRRC filter and the low-PAPR filter for QPSK and 16-QAM modulation schemes. As mentioned in the previous section, different filter shpes are obtained for different modulation schemes due to the effect of κ. Roll-off factor (α) is also considered.

Table 1 Simulation parameters.

Transmitter	Modulation	QPSK, 16QAM
	No. of symbols per block	$M = 256$
	FFT/IFFT block size	$N_c = 512$
	Cyclic prefix length	$N_g = 16$
Transmit filtering	Filter type	SRRC, Low-PAPR
	Roll-off factor	$\alpha = 0 \sim 1$
Optimization parameter	step-size	$\gamma = 1.0$
	No. of iterations	100
Channel	Fading type	Frequency-selective block Rayleigh
	Power delay profile	symbol-spaced 16-path uniform
Receiver	Equalizer	Joint MMSE-FDE w/ spectrum combining
	Channel estimation	Ideal

(a) SRRC filter

(b) Low-PAPR filter (QPSK)

(c) Low-PAPR filter (16-QAM)

Fig. 4 Filter transfer functions.

It can be observed from the figure that the shapes of low-PAPR filter obtained from Eq. (20) are a bit changed from SRRC filter shapes, especially when $\alpha \geq 0.5$. At the place that $\alpha \geq 0.75$ in low-PAPR filter for QPSK modula-
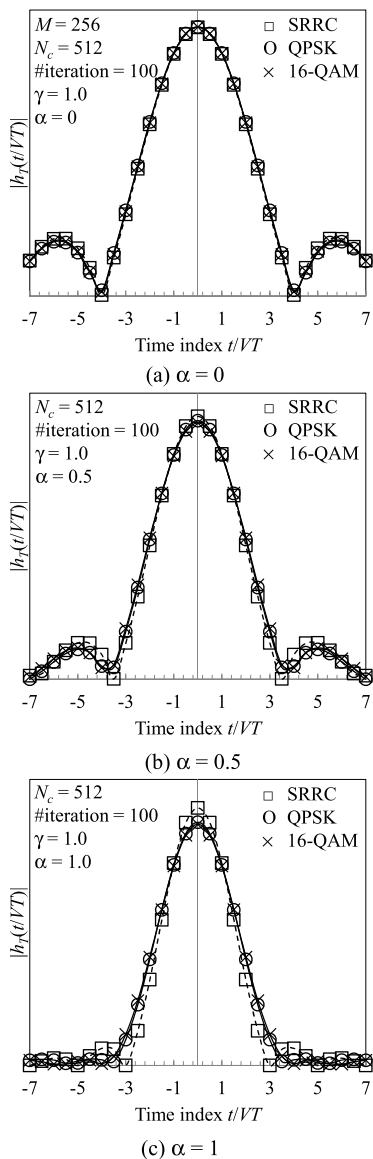
(a) $\alpha = 0$

(b) $\alpha = 0.5$

(c) $\alpha = 1$

Fig. 5 Filter impulse responses.

the proposed filter. Note that the effect of sidelobe of filter impulse response on PAPR is well described in Ref. [17], which confirms our results. We can also observe that peaks of the pulses are also reduced in the proposed filters.

It is observed from Figs. 4(b) and 4(c) that there exists spectrum increase at both edges, which is clearly visible when roll-off factor increases. We would like to describe this phenomenon by firstly showing how the gradient search algorithm affects the filter for the given number of iterations. Filter transfer functions and corresponding impulse responses of low-PAPR filter with $\alpha=1$ for 16-QAM modulation at the i-th iteration ($i=0$, 50, 100) are shown in Fig. 6, for describing how the iterative gradient search algorithm in Sect. 4 affects filter transfer function and impulse response. Here, we assume $M=128$, $N_c=256$, and oversampling factor $V=8$.

By referencing [17], [19], peak power reduction of transmit signal is due to the following reasons: sidelobe amplitude reduction, sidelobe misalignment, and pulse widening for reducing a peak occuring from pulse overlapping. Note that the terminology "sidelobe misalignment" is previously used in Ref. [19], and refers to an irregular alignment where zero-crossing of filter impulse response is not located at the sampling period (i.e. nt/T where n is integer and T is sampling period). Figure 6(b) confirms that the three abovementioned reasons of peak power reduction are gradually obvious when the number of iterations increases. It is also observed that the filter transfer function is "compressed" from the both sides of frequency spectrum when the number of iterations increases in order to obtain the corresponding impulse response in Fig. 6(b).

However, when the gradient search algorithm attemps to compress the frequency spectrum from the both sides, it leads to two possible alterations on filter transfer function, which corresponds to each other. One is an increasing around the center of transfer function, which occurs in every roll-off factors and modulation schemes (see Fig. 4(b) and 4(c)). Another one is alteration at the edges of filter transfer function. Figure 6(a) shows that the filter coefficients at the edges of transfer function gradually increase when the number of iterations increases. This is because the filter coefficients with low value at the edges of filter transfer function are pushed to negative region (i.e. $H_{T,opt}<0$), however, this region is converted to positive values instead due to the constraint of non-negative frequency-domain filter coefficients in Eq. (20). In addition, it is also observed that this phenomenon does not occur when α is low because the filter coefficients at the edges are relatively high compared to the filter with large α, hence the coefficients remain non-negative even though the transfer function is gradually compressed during the gradient search algorithm.

The occurrence of compressing the filter coefficients to negative region may imply that the constraint $H_T(k) \geq 0, \forall k$ should be relaxed. But it is confirmed by computer simulation that the low-PAPR filter with negative frequency-domain filter coefficients provides a slightly higher PAPR compared to the one with non-negative frequency-domain
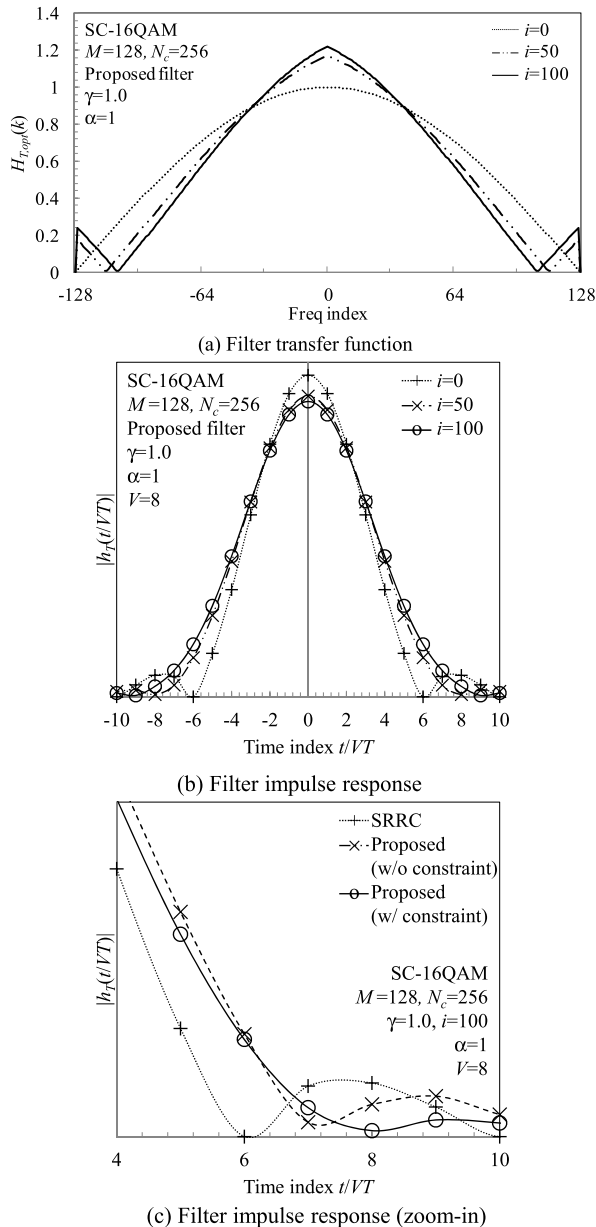
tion ($\alpha \geq 0.5$ for 16-QAM), there exist small lobes beside the main part of filters. To examine how these filter shapes can reduce the PAPR, time-domain filter impulse response should be available.

Figure 5 provides the time-domain filter impulse responses corresponding to the transfer functions shown in Fig. 4. The figures show comparison of various impulse responses of different filters at the same roll-off factor $\alpha=0$, 0.5, and 1. SRRC filter itself does not satisfy the Nyquist criterion, but a concatenation of SRRC at a transmitter and that at a receiver (which is equivalent to raised cosine filter) meets the Nyquist criterion. Therefore, the zero-crossing sampling timing is different when roll-off factor changes. It can be observed from the figures that the low-PAPR proposed filter, both for QPSK and 16-QAM, has lower sidelobe amplitude than SRRC filter. The reducion of sidelobe amplitude can be claimed as a reason of PAPR reduction of

(a) Filter transfer function

(b) Filter impulse response

(c) Filter impulse response (zoom-in)

Fig. 6 Filter transfer functions and corresponding impulse responses at particuar iterations.
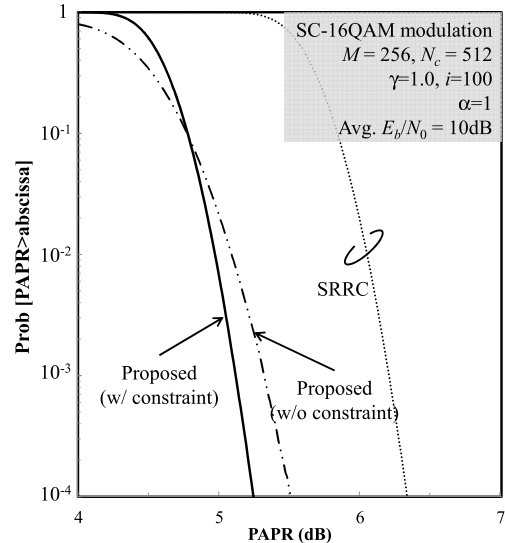

Fig. 7 PAPR the low-PAPR proposed filter with and without non-negative constraint (assuming $\alpha=1$).

(which is a zoom-in version of Fig. 6(b)) that the transmit impulse response obtained from the gradient search without constraint $H_T(k){\geq}0$ has a slight higher sidelobe compared to the one obtained from the gradient search with constraint. Even though this performance gap is very small (0.2 dB = 4.7% difference), the reason of this gap has been discussed as follows.

As discussed in Sect. 4.1, the gradient search algorithm reaches the same local minima as long as $H_T(k){\geq}0$. However, a gradient search algorithm which allows the negative transmit filter coefficients may lead to another local minima even if the same starting point, the same step-size parameter, and the same iterations are employed. It is confirmed by computer simulation assuming a block transmission consisting of 256 16-QAM-modulated symbols that a gradient search algorithm which allows the negative transmit filter coefficients reaches the same local minima as a gradient search algorithm with constraint $H_T(k){\geq}0$ at the 200th iteration with step-size $\gamma{=}0.5$ when $\alpha{=}1$. Note that the gradient search algorithm with constraint $H_T(k){\geq}0$ is conducted with the number of iterations = 100 and step-size $\gamma{=}1.0$ for every roll-off factor.
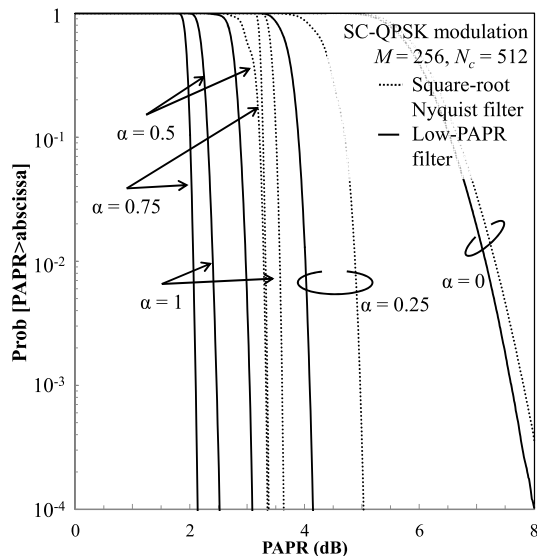
5.2 PAPR Performance

In this paper, PAPR calculation over a block of transmission is defined as
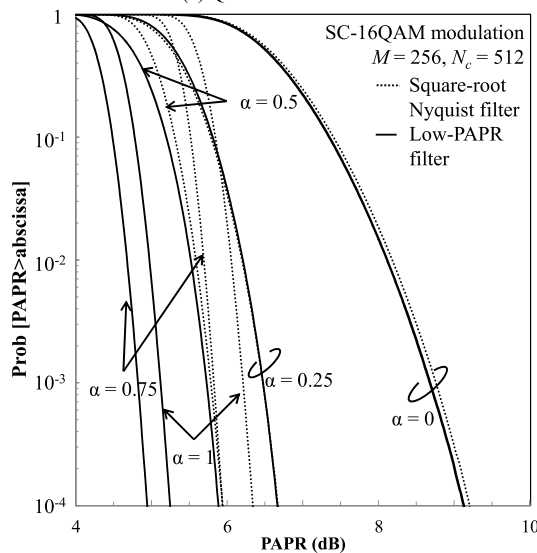
$$\text{PAPR} = \frac{\max[|s(n)|^2], n = 0, \frac{1}{V}, \frac{2}{V}, \ldots, N_c - 1}{E[|s(n)|^2]}, \quad (29)$$

where V represents oversampling factor (we consider $V{=}8$ in this paper). PAPR is evaluated by examining the CCDF.

Figure 8 shows the CCDF of PAPR of a comparison between transmissions using the low-PAPR proposed filtering and SRRC filtering, for both QPSK and 16-QAM modulation schemes. Roll-off factor α is also applicable. It is

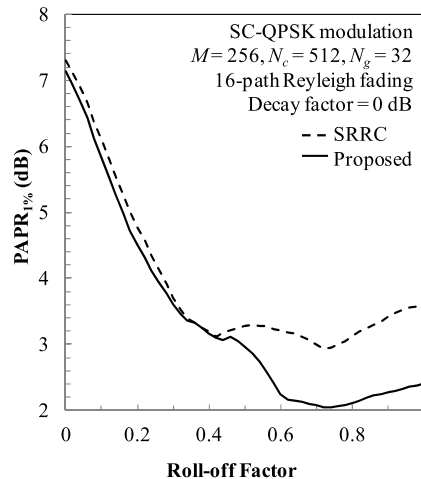filter coefficients due to an increasing of sidelobe magnitude, even though the same BER can be achieved.

We have evaluated the PAPR performance when using the transmit filter coefficients obtained from the gradient search algorithm with and without the constraint condition $H_T(k){\geq}0$. Figure 7 shows the simulation result of transmit PAPR using the proposed filtering with the roll-off factor $\alpha{=}1$ and 16-QAM. It is show that the use of the transmit filter coefficients obtained from the gradient search algorithm with constraint $H_T(k){\geq}0$ provides 0.2 dB lower PAPR than the one without constraint. The difference among PAPR performances with different values of α has also been discussed by examining the time-domain impulse responses of the resulting transmit filter coefficients. It is seen Fig. 6(c)

(a) QPSK modulation

(b) 16-QAM modulation

Fig. 8 CCDF of PAPR.

(a) QPSK modulation

(a) 16-QAM modulation

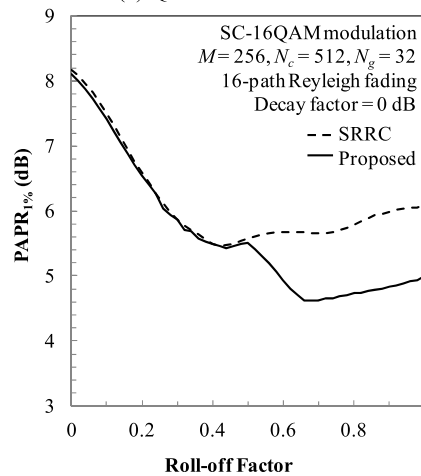**Fig. 9** $PAPR_{1\%}$ as a function of roll-off factor.

obviously seen from the figure that the PAPR of transmission using the proposed transmit filtering is lower than using SRRC filtering in every α.

At the place where probability of occurrence equals 0.1% ($PAPR_{0.1\%}$), approximately 0.3 dB (0.2 dB) reduction of PAPR is obtained when $\alpha=0$ for QPSK (16-QAM) modulation, while about 1.3 dB (1.0 dB) reduction is achievable when $\alpha=0.75$. We also would like to mention that the min-VIP problem in Eq. (20) is non-convex, and hence provides many points of local minima. Even though the gradient search algorithm in Eq. (26) cannot guarantee the global minimum, we can still achieve such a satisfactory PAPR result.

As it can be observed in both transmission schemes that the lowest PAPR is achieved at a particular α, we also evaluate the PAPR performance as a function of roll-off factor

α. Figure 9 shows the PAPR at a probability of occurrence of 1% ($PAPR_{1\%}$) of each transmission scheme as a function of α. From the figure, the lowest $PAPR_{1\%}$ of transmission using SRRC filtering is obtained when α is approximately 0.4 for both modulation schemes. The lowest $PAPR_{1\%}$ of the transmission using the proposed low-PAPR transmit filtering is achieved when α is about 0.75 for QPSK and 0.65 for 16-QAM. We can also observe that the proposed filtering gives better PAPR improvement when α is higher than 0.4.

5.3 BER Performance

BER performance of SC-FDE transmission using each transmit filtering is shown in Fig. 10 as a function of average received energy-to-noise power spectrum density ratio $E_b/N_0 = (1/N_{mod})(E_s/N_0)(1+N_g/N_c)$ where N_{mod} represents modulation level (2 for QPSK and 4 for 16-QAM). Performance evaluation is done for roll-off factor $\alpha=0$, 0.5, and 1. As α increases, the BER performance improves due to higher frequency diversity gain resulting from joint MMSE-
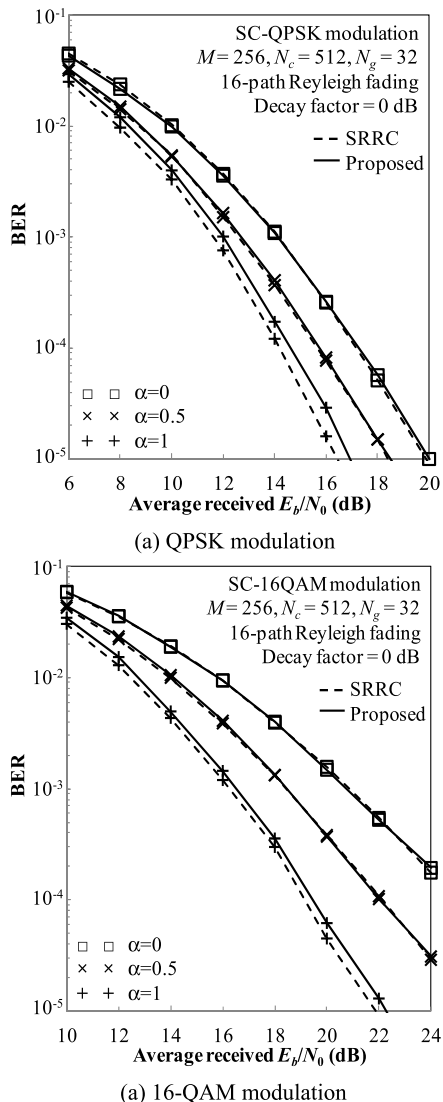
(a) QPSK modulation

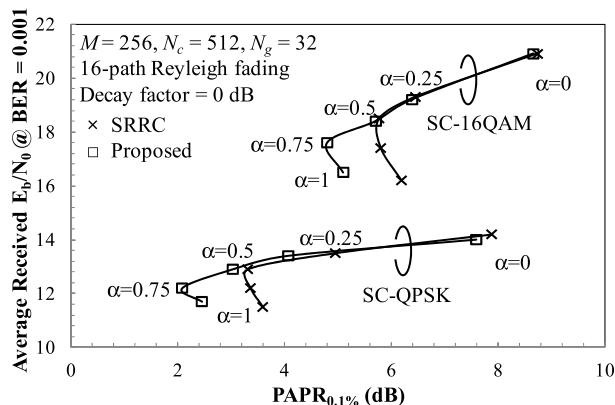(a) 16-QAM modulation

Fig. 10 BER performance.

Fig. 11 Performance tradeoff.

BER=10^{-3}, as shown in Fig. 11. It can be observed for both QPSK and 16-QAM modulation schemes that SC-FDE using the proposed low-PAPR transmit filtering provides better PAPR where the required transmit power for achieving particular BER is not changed, as the performance tradeoff curve shifts to the left.

6. Conclusion

A new low-PAPR transmit filtering based on min-VIP criterion for SC-FDE was designed in this paper. The proposed transmit filtering can achieve excess-bandwidth transmission by changing the roll-off factor. A combination of the proposed filtering and joint MMSE-FDE and spectrum combining provides additional frequency diversity gain through the excess-bandwidth in a frequency-selective channel. Simulation results confirmed that the proposed low-PAPR transmit filtering gives lower PAPR with only a slight BER performance degradation compared to the SRRC filtering.

References

[1] D. Astely, E. Dahlman, A. Furusskar, Y. Jading, M. Lindstorm, and S. Parkvall, "LTE: The evolution of mobile broadband," IEEE Commun. Mag., vol.47, no.4, pp.44–51, April 2009.

[2] A. Goldsmith, Wireless Communications, Cambridge University Press, 2005.

[3] S.H. Han and J.H. Lee, "An overview of peak-to-average power ratio reduction techniques for multicarrier transmission," IEEE Trans. Wireless Commun., vol.12, no.2, pp.56–65, April 2005.

[4] D. Falconer, S.L. Ariyavisitakul, A. Benyamin-Seeyar, and B. Edison, "Frequency domain equalization for single-carrier broadband wireless systems," IEEE Commun. Mag., vol.40, no.4, pp.58–66, April 2002.

[5] H. Sari, G. Karam, and J. Jeanclaude, "Transmission techniques for

FDE and spectrum combining.

There exists the similarity between the BER performances of QPSK and 16-QAM modulations. When α=0 and 0.5, the BER performance with the SRRC filtering and that with the proposed filtering are almost the same. When α=1, the BER performance with the proposed filtering is only slightly worse (less than 0.4 dB) than that with the SRRC filtering. A possible reason behind the above result is discussed in Appendix-D.

It is a fact that the proposed transmit filter does not satisfy the Nyquist criterion. However, a concatenation of transmit filter and the FDE at the receiver acts based on the MMSE criterion to satisfy the Nyquist criterion. The simulation results confirm that the BER performances at roll-off factor α=0 and 0.5 are almost the same and are only slightly degraded from the case of SRRC when α=1.

Finally, we also provide a performance tradeoff curve between PAPR$_{0.1\%}$ and the required E_b/N_0 for achieving

digital terrestrial TV broadcasting," IEEE Commun. Mag., vol.33, no.2, pp.100–109, Feb. 1995.

[6] H. Wu and T. Haustein, "Radio resource management for the multiuser uplink using DFT-precoded OFDM," Proc. IEEE International Conf. on Commun. (ICC 2008), pp.4724–4728, Beijing, China, May 2008.

[7] K. Takeda and F. Adachi, "Joint iterative transmit/receive FDE&FDIC for single-carrier block transmissions," IEICE Trans. Commun., vol.E94-B, no.5, pp.1396–1404, May 2011.

[8] Y. Akaiwa, Introduction to Digital Mobile Communication, 1st ed., Wiley, 1997.

[9] S. Daumont, B. Rihawi, and Y. Lout, "Root-raised cosine filter influents on PAPR distribution of single carrier signals," Proc. 3rd International Symposium on Commun., Control and Signal Processing (ISCCSP 2008), pp.841–845, St. Julians, Malta, March 2008.

[10] T. Obara, K. Takeda, and F. Adachi, "Joint frequency-domain equalization and spectrum combining for the reception of SC signals in the presence of timing offset," Proc. IEEE Vehicular Tech. Conference (VTC) 2010-Spring, pp.1–5, Taipei, Taiwan, May 2010.

[11] S. Okuyama, K. Takeda, and F. Adachi, "MMSE frequency-domain equalization using spectrum combining for Nyquist filtered broadband single-carrier transmission," Proc. IEEE Vehicular Tech. Conference (VTC) 2010-Spring, pp.1–5, Taipei, Taiwan, May 2010.

[12] N.C. Beaulieu, C.C. Tan, and M.O. Damen, "A better-than Nyquist pulse," IEEE Commun. Lett., vol.5, no.9, pp.367–368, Sept. 2001.

[13] P. Rha and S. Hsu, "Peak-to-average ratio (PAR) reduction by pulse shaping using a new family of generalized raised cosine filter," Proc. IEEE Vehicular Tech. Conference (VTC) 2003-Fall, pp.706–710, Florida, USA, Oct. 2003.

[14] C. Meza, K. Lee, and K. Lee, "PAPR reduction in single carrier FDMA uplink system using parametric linear pulses," Proc. 2011 International Conference on ICT Convergence (ICTC 2011), pp.424–429, Seoul, Korea, Sept. 2011.

[15] S. Chandan, P. Sandeep, and A. Chaturvedi, "A family of ISI-freePolynomial pulses," IEEE Commun. Lett., vol.9, no.6, pp.496–498, June 2005.

[16] S. Mohapatra and S. Das, "Peak-to-Average Power Reduction (PAPR) by pulse shaping using a modified raised cosine filters," Proc. 2009 Annual IEEE India Conference (INDICON 2009), pp.1–4, Gandhinagar, India, Dec. 2009.

[17] S. Slimane, "Reducing the peak-to-average power ratio of OFDM signals through precoding," IEEE Trans. Veh. Technol., vol.56, no.2, pp.686–695, March 2007.

[18] D. Falconer, "Linear precoding of OFDMA signals to minimize their instantaneous power variance," IEEE Trans. Commun., vol.59, no.4, pp.1154–1162, April 2011.

[19] C.H. Yeun and B. Farhang-Boroujeny, "Analysis of the optimum precoder in SC-FDMA," IEEE Trans. Commun., vol.11, no.11, pp.4096–4107, Nov. 2012.

[20] A. Papoulis and S.U. Pollai, Probability, Random Vairables and Stochastic Processes, 4th ed., McGraw-Hills, 2002.

[21] S. Boyd and L. Vandenberghe, Convex Optimization, Cambridge University Press, 2004.

[22] A. Ben-Israel and T.N.E. Greville, Generalized Inverses: Theory and Applications, 2nd ed., Wiley, 2003.

[23] K. Takeda and F. Adachi, "Joint transmit/receive one-tap minimum mean square error frequency-domain equalization for broadband multicode direct-sequence code division multiple access," IET Commun., vol.4, no.14, pp.1752–1764, Sept. 2010.

[24] A. Boonkajay, T. Obara, T. Yamamoto, and F. Adachi, "Frequency-domain single-carrier spread spectrum with joint FDE and spectrum combining," Proc. International Conference on Information, Communs. and Signal Processing (ICICS 2013), pp.1–5, Tainan, Taiwan, Dec. 2013.

Appendix A: Derivarion of VIP Formula in Eq. (18)

The derivation begins from Eq. (17) as

$$\sigma^2 = \frac{1}{N_c} \sum_{n=0}^{N_c-1} E[|s(n)|^4] - P_{avg}^2. \tag{A·1}$$

Then, substitute Eq. (15) into Eq. (A·1) yields

$$\sigma^2 = \frac{1}{N_c} \sum_{n=0}^{N_c-1} \left(E\left[\left| \sum_{m=0}^{M-1} x_{nm} d(m) \right|^4 \right] - P_{avg}^2 \right). \tag{A·2}$$

By considering all of the transmit symbols $d(m)$ are independent, distributing the fourth-order term yields

$$\sigma^2 = \frac{1}{N_c} \sum_{n=0}^{N_c-1} \left(E\left[\left| \sum_{m=0}^{M-1} x_{nm} d(m) \right|^4 \right] - P_{avg}^2 \right)$$
$$= \frac{1}{N_c} \sum_{n=0}^{N_c-1} \left(E\left[\sum_{m=0}^{M-1} |x_{nm}|^4 |d(m)|^4 \right] - P_{avg}^2 \right.$$
$$\left. + 2E\left[\sum_{m=0}^{M-1} |x_{nm}|^2 |d(m)|^2 \sum_{m'=0,m'\neq m}^{M-1} |x_{nm'}|^2 |d(m')|^2 \right] \right) \tag{A·3}$$

Here, $E[|d(m)|^2]=1$ for both QPSK and 16-QAM modulation, but $E[|d(m)|^4] \neq 1$ for 16-QAM. Substituting $E[|d(m)|^2]=1$ into Eq. (A·3) and eliminating the ensemble average terms yields

$$\sigma^2 = \frac{1}{N_c} \sum_{n=0}^{N_c-1} \left(E\left[|d(m)|^4 \right] \sum_{m=0}^{M-1} |x_{nm}|^4 - P_{avg}^2 \right.$$
$$\left. + 2\left[\sum_{m=0}^{M-1} |x_{nm}|^2 \sum_{m'=0,m'\neq m}^{M-1} |x_{nm'}|^2 \right] \right)$$
$$= \frac{1}{N_c} \sum_{n=0}^{N_c-1} \left(E\left[|d(m)|^4 \right] \sum_{m=0}^{M-1} |x_{nm}|^4 - P_{avg}^2 \right.$$
$$\left. + 2\left[\sum_{m=0}^{M-1} \left[|x_{nm}|^2 \right]^2 - \sum_{m=0}^{M-1} |x_{nm}|^4 \right] \right) \tag{A·4}$$

After rearranging some terms, we obtain

$$\sigma^2 = \frac{1}{N_c} \sum_{n=0}^{N_c-1} \left[2\left[\sum_{m=0}^{M-1} |x_{nm}|^2 \right]^2 - (2-\kappa) \sum_{m=0}^{M-1} |x_{nm}|^4 \right] - P_{avg}^2. \tag{A·5}$$

where $\kappa = E[|d(m)|^4]$. Note that in case of QPSK, Eq. (A·5) is simplified as

$$\sigma^2 = \frac{1}{N_c} \sum_{n=0}^{N_c-1} \left[2\left[\sum_{m=0}^{M-1} |x_{nm}|^2 \right]^2 - \sum_{m=0}^{M-1} |x_{nm}|^4 \right] - P_{avg}^2 \tag{A·6}$$

Appendix B: Derivation of Gradient Function of VIP
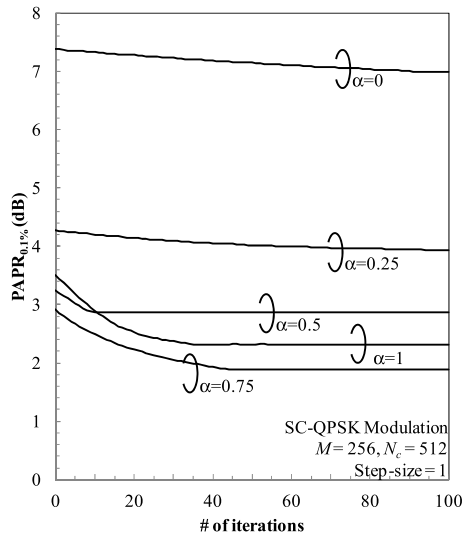
The derivation begins from Eq. (22) as

Fig. A·1   Convergence of gradient search algorithm after 100 iterations.

$$\nabla_{\mathbf{p}_m}\sigma^2 = \nabla_{\mathbf{p}_m,\text{real}}\sigma^2 + j\nabla_{\mathbf{p}_m,\text{img}}\sigma^2. \tag{A·7}$$

Using Eq. (18) and applying the partial derivative, Eq. (A·7) is rewritten as

$$\nabla_{\mathbf{p}_m}\sigma^2 = \frac{1}{N_c}\sum_{n=0}^{N_c-1}\left[\frac{\partial}{\partial\mathbf{p}_m}\left(2\left[\sum_{m=0}^{M-1}|x_{nm}|^2\right]^2\right)\right.$$
$$\left. -(2-\kappa)\frac{\partial}{\partial\mathbf{p}_m}\left(\sum_{m=0}^{M-1}|x_{nm}|^4\right)\right] \tag{A·8}$$

We can observe that x_{nm} is a dot product of the n-th column vector of $\mathbf{F}_{N_c}^H$, representing by $\mathbf{e}_n$, and $\mathbf{p}_m$. Therefore, Eq. (A·8) can be rearranged as follows.

$$\nabla_{\mathbf{p}_m}\sigma^2 = \frac{1}{N_c}\sum_{n=0}^{N_c-1}\left[4\left[\sum_{l=0}^{M-1}|x_{nl}|^2\right]^2(2x_{nm}\mathbf{e}_n^H)-(2-\kappa)(4|x_{nm}|^3\mathbf{e}_n^H)\right]$$
$$= \frac{4}{N_c}\sum_{n=0}^{N_c-1}\left[\left[\sum_{l=0}^{M-1}|x_{nl}|^2\right]^2(2x_{nm}\mathbf{e}_n^H)-(2-\kappa)(x_{nm}|x_{nm}|^2\mathbf{e}_n^H)\right]$$
$$= \frac{4}{N_c}\sum_{n=0}^{N_c-1}\left[2\left(\left[\sum_{l=0}^{M-1}|x_{nl}|^2\right]^2\right)-(2-\kappa)(|x_{nm}|^2)\right](x_{nm}\mathbf{e}_n^H) \tag{A·9}$$

where $\mathbf{e}_n$ is already defined in Eq. (25).

Appendix C: Convergence Analysis of Gradient Search Algorithm

To examine the convergence, the $PAPR_{0.1\%}$ is plotted as the number of iterations in Fig. A·1. The step-size $\gamma=1.0$ was used following Ref. [18]. It can be seen from Fig. A·1 that when $\alpha=0.5$, 0.75, and 1, the PAPR reduction can be converged before 100 iterations while more iterations are necessary to converge when $\alpha=0$ and 0.25. Hpwever, since the PAPR can be only slightly reduced when $\alpha=0$ and 0.25, the

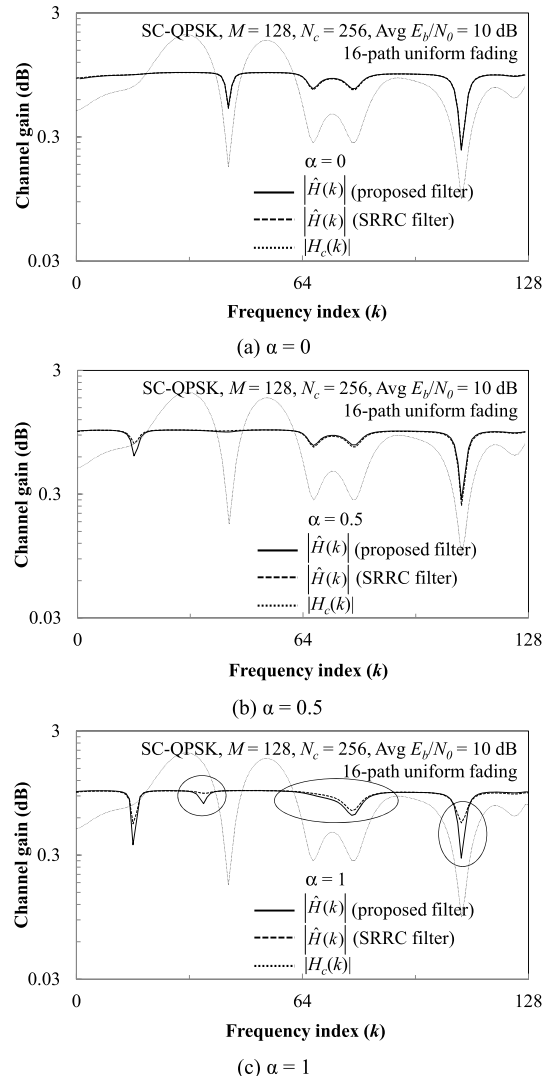(a) α = 0

(b) α = 0.5

(c) α = 1

Fig. A·2   Frequency-domain equivalent channel response of transmission using SRRC and the proposed filtering.

iterative gradient search algorithm was designed to stop at the 100th iteration.

Appendix D: Equivalent Channel Response After Joint MMSE-FDE and Spectrum Combining

The equivalent channel response [23], [24] is introduced. From Eqs. (10) and (14), the equivalent channel $\hat{\mathbf{H}} = diag\left[\hat{H}(0),\hat{H}(1),\ldots,\hat{H}(M-1)\right]$ is given by

$$\hat{\mathbf{H}} = \mathbf{W}\mathbf{H}_c\mathbf{H}_T. \tag{A·10}$$

where $\mathbf{H}_c$ and its k-th diagonal element, $H_c(k)$, are defined in Eq. (11). Substituting Eq. (A·10) into Eq. (14), the received signal before demodulation $\hat{d}(m)$, associated with the m-th transmitted symbol, can be expressed as

$$\hat{d}(m) = \sqrt{\frac{2E_s}{T_s}}\left(\frac{1}{M}\sum_{k=0}^{M-1}\hat{H}(k)\right)d(m)$$

$$+ \sqrt{\frac{2E_s}{T_s}} \left(\frac{1}{M} \sum_{k=0}^{M-1} \hat{H}(k) \sum_{\tau=0, \tau \neq t}^{M-1} d(\tau) \exp\left(j2\pi k \frac{t-\tau}{M} \right) \right)$$

$$+ \frac{1}{M} \sum_{k=0}^{M-1} \hat{N}(k) \exp\left(j2\pi k \frac{t}{M} \right) \tag{A.11}$$

where $\hat{N}(k)$ is the noise after MMSE-FDE and spectrum combining. According to Ref. [24], the conditional instantaneous signal-to-interference plus noise power ratio (SINR) for the given average received E_s/N_0 and channel $\mathbf{H}_c$ is given by

$$\gamma\left(\frac{E_s}{N_0}, \mathbf{H}_c \right)$$

$$= \frac{\frac{2E_s}{N_0} \left| \frac{1}{M} \sum_{k=0}^{M-1} \hat{H}(k) \right|^2}{\left(\frac{1}{M} \sum_{k=0}^{N_c-1} |W(k)|^2 + \frac{E_s}{N_0} \left(\frac{1}{M} \sum_{k=0}^{M-1} \left| \hat{H}(k) \right|^2 - \left| \frac{1}{M} \sum_{k=0}^{M-1} \hat{H}(k) \right|^2 \right) \right)} \tag{A.12}$$

The second term of the denominator of Eq. (A.12) is the variance of $\hat{H}(k)$ and represents the residual inter-symbol interference (ISI) power. The BER is a monotonically decreasing function of the conditional SINR [24]. This means that the equivalent channel response should be made flat as much as possible.

We have examined the one-shot observation the equivalent channel responses of SC-QPSK transmission using SRRC transmit filtering and that using the proposed filtering for various values of α when the average received $E_b/N_0 = 10$ dB. A one-shot observation of the equivalent channel response assuming $M = 128$ and QPSK modulation is provided in Fig. A.2. From Fig. A.2, it can be observed that when $\alpha = 0$ and 0.5, the equivalent channel response with the SRRC transmit filtering and that with the proposed transmit filtering are almost the same. Therefore, two filtering techniques provide almost the same conditional SINR, thereby providing almost the same BER performance. However, when $\alpha = 1$, the proposed transmit filtering is seen to have slightly higher variations in the equivalent channel response than the SRRC filtering; therefore, the proposed filtering provides slightly lower conditional SINR, thereby providing a worse BER performance.

Amnart Boonkajay received his B.S. degree in Telecommunication Engineering from Sirindhorn International Institute of Technology, Thailand, and M.S. degree in Electrical and Communication Engineering from Tohoku University, Japan, in 2010 and 2013, respectively. Currently he is studying toward PhD degree at the Department of Communications Engineering, Graduate School of Engineering, Tohoku University. His research interests include frequency-domain baseband signal transmit and receive processing, filtering, and equalization techniques for next-generation mobile communication systems.

Tatsunori Obara received his B.S. degree in Electrical, Information and Physics Engineering in 2008 and M.S. degree in communications engineering, in 2010, respectively, from Tohoku University, Sendai Japan. Currently he is a Japan Society for the Promotion of Science (JSPS) research fellow, studying toward his PhD degree at the Department of Electrical and Communications Engineering, Graduate School of Engineering, Tohoku University. His research interests include channel equalization techniques for mobile communication systems.

Tetsuya Yamamoto received his B.S. degree in Electrical, Information and Physics Engineering in 2008 and M.S. and Dr. Eng. degrees in communications engineering from Tohoku University, Sendai Japan, in 2010 and 2012, respectively. From April 2010 to March 2013, he was a Japan Society for the Promotion of Science (JSPS) research fellow. Since April 2013, he has been with Panasonic Corporation. He was a recipient of the 2008 IEICE RCS (Radio Communication Systems) Active Research Award and Ericsson Best Student Award 2012.

Fumiyuki Adachi received the B.S. and Dr. Eng. degrees in electrical engineering from Tohoku University, Sendai, Japan, in 1973 and 1984, respectively. In April 1973, he joined the Electrical Communications Laboratories of Nippon Telegraph & Telephone Corporation (now NTT) and conducted various types of research related to digital cellular mobile communications. From July 1992 to December 1999, he was with NTT Mobile Communications Network, Inc. (now NTT DoCoMo, Inc.), where he led a research group on wideband/broadband CDMA wireless access for IMT-2000 and beyond. Since January 2000, he has been with Tohoku University, Sendai, Japan, where he is a distinguished Professor of Communications Engineering at the Graduate School of Engineering. His research interest is in the areas of wireless signal processing and networking including broadband wireless access, equalization, transmit/receive antenna diversity, MIMO, adaptive transmission, channel coding, etc. He was a program leader of the 5-year Global COE Program "Center of Education and Research for Information Electronics Systems" (2007–2011), awarded by the Ministry of Education, Culture, Sports, Science and Technology of Japan. From October 1984 to September 1985, he was a United Kingdom SERC Visiting Research Fellow in the Department of Electrical Engineering and Electronics at Liverpool University. He is an IEICE Fellow and was a co-recipient of the IEICE Transactions best paper of the year award 1996, 1998, and 2009 and also a recipient of Achievement award 2003. He is an IEEE Fellow and a VTS Distinguished Lecturer for 2011 to 2013. He was a co-recipient of the IEEE Vehicular Technology Transactions best paper of the year award 1980 and again 1990 and also a recipient of Avant Garde award 2000. He was a recipient of Thomson Scientific Research Front Award 2004, Ericsson Telecommunications Award 2008, Telecom System Technology Award 2009, and Prime Minister Invention Prize 2010.